Research Article

Journal of Environmental Nanotechnology

Green Synthesis of ZnO Nanoparticles Using *Azadirachta indica* Leaf Extract for Rapid Catalytic Degradation of Organic Pollutants

Ashvin B Amale[1], P. Satishkumar[2*], Pramod Rambhau Bhagat[3], Manoj S. Motghare[4] and C. Krishnaraj[5]

[1]Department of Mechanical Engineering, Yeshwantrao Chavan College of Engineering, Nagpur, MH, India
[2]Department of Mechanical Engineering, Rathinam Technical Campus, Coimbatore, TN, India
[3]Department of Mechanical Engineering, St. Vincent Pallotti College of Engineering and Technology, Nagpur, MH, India
[4]Department of Mechanical Engineering, Govindrao Wanjari College of Engineering and Technology, Nagpur, MH, India
[5]Department of Mechanical Engineering, Rathinam Technical Campus, Coimbatore, TN, India
[6]Department of Engineering, University of Technology and Applied Sciences, Nizwa, Oman
Received: 18.02.2026 Accepted: 21.03.2026 Published: 30.06.2026
*spsatishkumar1986@gmail.com

ABSTRACT

Green synthesis of zinc oxide nanoparticles (ZnO NPs) using plant extracts provides an environmentally sustainable alternative to conventional chemical synthesis methods. In this study, ZnO NPs were synthesized using *Azadirachta indica* leaf extract and characterized using X-ray diffraction (XRD), UV–visible spectroscopy, Fourier transform infrared spectroscopy (FTIR), dynamic light scattering (DLS), scanning electron microscopy (SEM), and energy dispersive X-ray spectroscopy (EDX). The synthesized nanoparticles exhibited uniform morphology with particle sizes below 100 nm. The catalytic performance of ZnO nanoparticles was evaluated for the degradation of organic dyes including methyl orange (MO), methylene blue (MB), and Congo red (CR). The results demonstrated high degradation efficiencies of 95.35% for MO, 97.82% for MB, and 98.29% for CR within short reaction times. In addition, the ZnO NPs efficiently catalyzed the reduction of *p*-nitrophenol to *p*-aminophenol within 2–4 minutes in the presence of $NaBH_4$. The enhanced catalytic activity is attributed to the high surface area and active sites of the biosynthesized ZnO nanoparticles. These findings demonstrate that neem-mediated ZnO nanoparticles offer a cost-effective, rapid, and environmentally friendly catalytic system for the remediation of dye-contaminated wastewater.

Keywords: *Azadirachta indica* leaf; ZnO nanoparticles; *p*-Aminophenol; Congo red; Methyl orange.

1. INTRODUCTION

The primary industries utilizing dyestuffs and colorants as textiles, paper, paints, food and pulp. Synthetic dyes released from textile, paper, paint, and food industries constitute a major source of water pollution due to their complex aromatic structures and resistance to biodegradation. Therefore, the development of efficient and sustainable catalytic systems for dye degradation has become an important research focus.

Green synthesized ZnO demonstrated stronger cytotoxicity than chemically synthesized counterparts (Rani et al., 2022). ZnO nanoparticle characterized by SEM-EDX, XRD and TEM enabled catalytic synthesis of bioactive steroidal compounds. Moderate-to-good antioxidant increased with concentration (Ansari *et al.* 2022). Ag–ZnO nanocomposites showed reduced bandgap and confirmed crystallinity by XRD and SEM. Linear I–V characteristics indicated good electrical conductivity. Enhanced photocatalytic and antibacterial performance was reported (Slathia *et al.* 2021). ZnO-based composites (average size 108.3 ± 73.4 nm) were characterized by FE-SEM and EDX. Effective dye removal was achieved for methylene blue and Congo red. Antibacterial inhibition were observed against S. aureus and *P. aeruginosa*. (Doan *et al.* 2025).

Green synthesized ZnO NPs showed hexagonal zincite structure confirmed by XRD and controlled morphology by SEM/TEM. Complete degradation (100%) of CR and MB was achieved under UV irradiation. At least 81% degradation was observed for rhodamine B, methyl orange and malachite green, (Fuentes *et al.* 2025). ZnO NPs exhibited a bandgap of 2.95 eV with crystallite size of 12.77 nm confirmed at XRD. Photocatalytic degradation of Congo red, methylene blue, rhodamine B, methyl orange, and malachite green occurred within 180 min. The nanoparticles demonstrated strong UV-driven catalytic efficiency (Magaña-Chavez *et al.* 2025). Zn-based NPs showed hexagonal and orthorhombic crystalline phases confirmed by XRD and SEM. Degradation of methyl orange, methylene blue and Congo red was reported under photocatalytic conditions. Strong antioxidant activity and antibacterial efficacy against *B. subtilis* were observed (Raza *et al.* 2025).

Hexagonal ZnO NPs were confirmed by HR-TEM, XRD, and SEM with UV peak at ~376 nm. Photodegradation of methyl orange, Congo red and methylene blue followed pseudo-first-order kinetics. High efficiency was achieved under natural sunlight conditions (Lal *et al.* 2024). ZnO NPs (18.25–36.88 nm) showed hexagonal zincite structure confirmed by XRD and Zn–O vibration at 560 cm^{-1} by FTIR. Strong photoluminescence peaks were observed at 425, 467, and 492 nm. Efficient degradation of five dyes occurred within 180 min (Barrios-Navarro *et al.* 2024). ZnO NPs (<20 nm) exhibited hexagonal wurtzite structure with Zn–O stretching at 397 cm^{-1}. Effective degradation was achieved for malachite green, Congo red and methylene blue. Methyl orange and rhodamine B showed comparatively slower degradation (Quevedo-Robles *et al.* 2024). ZnO NPs (<30 nm) showed a bandgap of 3.25 eV confirmed by UV-DRS and hexagonal phase via XRD. Photocatalytic degradation exceeded 98% for *p*-nitrophenol under UV-LED irradiation. Distinct quasi-spherical and nanorod morphologies were observed by SEM (Ounis *et al.* 2025).

$Fe_3O_4/ZrO_2/ZnO$ nanocomposite exhibited ~90% degradation of *p*-nitrophenol within 38 min under solar irradiation. The MIC values were 1.25 µg/mL (*S. aureus*) and 0.125 µg/mL (*E. coli*). The catalyst retained >80% efficiency after five cycles (Arayesh *et al.* 2023). Ti/Cu/Zn-HEG nanocomposite achieved 98.4% reduction of *p*-nitrophenol under optimized conditions (150 ppm, 400 ppm catalyst, 10 min). Regression coefficient $R^2 > 0.97$ confirmed strong model prediction accuracy. The catalyst showed high stability and reusability (Behera *et al.* 2023). Ag/ZnO-chitosan nanocomposites showed crystalline phases by XRD and uniform distribution by SEM-EDX. Pseudo-first-order rate constant for para-nitrophenol was 2.813×10^{-3} s^{-1} and 1.663×10^{-3} s^{-1} for methyl orange. The catalyst was recyclable without significant activity loss (Khan *et al.* 2022). ZnO/PpAP nanocomposites showed decreasing bandgap and increasing refractive index up to 7 wt% ZnO loading. The XRD studies confirmed uniform nanoparticle dispersion. Activation energy decreased with frequency, supporting thermally activated conduction (Furhan and Ramesan, 2023). PpAP/ZnO composites (≤7 wt%) showed enhanced dielectric constant and AC conductivity. The SEM analysis confirmed homogeneous nanoparticle growth in polymer matrix. The 7 wt% sample exhibited best ammonia sensing performance at room temperature (Furhan and Ramesan, 2022).

ZnO–NiO nanocomposite (~30 nm crystallite size) showed hexagonal ZnO and FCC NiO phases by XRD. Congo red degradation reached 79% under UV irradiation. SC was 120 F g^{-1} at 10 mV s^{-1} (Krishnaiah and Kumar, 2025). CuO–ZnO NCs (~20 nm) showed 79% degradation of Congo red under UV exposure. Bandgap energy was 3.37 eV. Specific capacitance was 31 F g^{-1} at 30 mV s^{-1} (Venkata and Behara, 2025). Doped hematite NPs (22.83 nm) achieved 97% methylene blue and 95% methyl orange degradation. The R^2 values ranged from 0.91–0.95 confirming pseudo-first-order kinetics. Photocatalytic activity remained stable after four cycles (Kumar *et al.* 2024). Nanoparticles (8.64–15.32 nm) showed 98.36% Eosin Yellow degradation and 96.42% Congo red. Saturation magnetization ranged from 36–45 emu g^{-1}. The DPPH inhibition ranged from 71.13% to 90.35% (Kumar and Thakur, 2025). Iron-loaded biochar achieved 89.7% Congo red degradation at pH 6 within 60 min. Optimal PMS concentration was 300 mg L^{-1}. Catalyst maintained activity over four cycles (Nandana *et al.* 2024). Activated bark carbon showed spontaneous and endothermic Congo red adsorption. Pseudo-second-order kinetics provided best fit. The SEM and FTIR studies confirmed surface modification after adsorption (Kumar *et al.* 2023). Bentonite–neem composite followed pseudo-second-order kinetics for Congo red adsorption. Freundlich isotherm best described adsorption behavior. The process was spontaneous and endothermic (Manzoor *et al.* 2023).

Despite extensive studies on plant-mediated synthesis of ZnO nanoparticles, many investigations mainly focus on either photocatalytic degradation or adsorption processes individually. Limited studies have systematically investigated the rapid catalytic reduction of multiple organic dyes together with nitroaromatic compound transformation using neem-mediated ZnO nanoparticles under $NaBH_4$-assisted conditions.

Among various plant extracts used for green synthesis, *Azadirachta indica* (neem) possesses abundant bioactive phytochemicals such as flavonoids, terpenoids, and polyphenols that act as natural reducing and stabilizing agents. These compounds enhance nanoparticle nucleation, improve surface functionalization, and promote efficient electron transfer during catalytic reactions. Consequently, neem-mediated ZnO nanoparticles often exhibit improved stability, smaller particle size, and enhanced catalytic activity compared with nanoparticles synthesized using several other plant extracts.

Although *Azadirachta indica* (neem) leaf extract has been widely employed for eco-friendly synthesis of ZnO NPs, comprehensive studies integrating rapid catalytic dye reduction and nitroaromatic compound transformation using neem-mediated ZnO under $NaBH_4$-assisted conditions remain relatively limited. In particular, the role of phytochemical surface functionalization in enhancing electron transfer during catalytic reduction processes requires further exploration. Therefore, the present study aims to synthesize ZnO nanoparticles by an eco-friendly route using *Azadirachta indica* leaf extract and to systematically evaluate their catalytic performance for reduction of azo dyes. Comprehensive characterization

using XRD, UV–Vis spectroscopy, FTIR, DLS, SEM, and EDX is performed to assess structural and morphological properties. The catalytic efficiency is assessed through kinetic modeling to determine pseudo-first-order rate constants and degradation efficiencies. This work highlights a sustainable, cost-effective, and rapid catalytic system for wastewater remediation using plant-mediated ZnO nanoparticles.

2. MATERIALS AND METHODOLOGY

2.1 Materials

Zinc nitrate hexahydrate ($Zn(NO_3)_2 \cdot 6H_2O$) was acquired from Matrics Enterprises in Nagercoil, Tamil Nadu, India, and utilized as the zinc precursor for manufacture of zinc oxide nanoparticles. *p*-Nitrophenol (PNP), ammonium hydroxide, methylene blue (MB), Congo red (CR), and Methyl orange (MO) were acquired from Star Scientific Enterprises in Erode. All solutions were prepared using pure water.

2.2 Preparation of Extract

Fresh *Azadirachta indica* leaves were harvested and meticulously rinsed twice with distilled water to remove surface contaminants and dust. Subsequently, 250 mL of deionized water were introduced at 1 L beaker holding the purified leaves and heated 80 °C for 90 minutes at constant agitation. Reaching room temperature, resultant extract were filtered using Whatman paper to eliminate solid residues (Khan *et al.* 2025a). The *Azadirachta indica* leaf extract was preserved at 10 °C in a refrigerator for the preparation of zinc oxide nanoparticles.

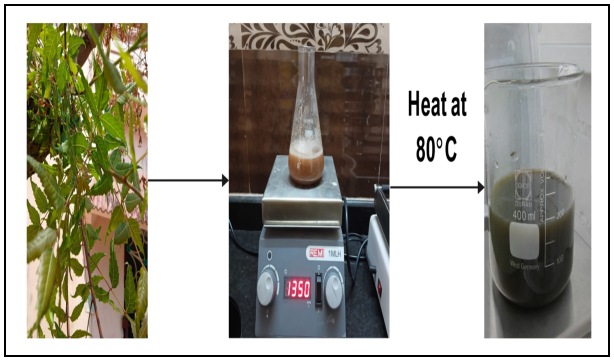


Fig. 1: Preparation steps of *Azadirachta indica* leaf extract

2.3 Synthesis of ZnO NPs

The synthesis was carried out under controlled laboratory conditions at room temperature (25 ± 2 °C). A zinc nitrate hexahydrate ($Zn(NO_3)_2 \cdot 6H_2O$, 30 mmol) were formulated at distilled water. To this solution, 0.2 mL of NH_4OH was incrementally added while continuous magnetic stirring at approximately 500 rpm for 60 minutes. The pH of the reaction mixture was adjusted using NH_4OH to facilitate the formation of $Zn(OH)_2$ precursor species prior to ZnO nanoparticle formation. Subsequently, 5 mL of *Azadirachta indica* leaf extract was gradually introduced to reaction mixture. The liquid was agitated continuously for one hour at ambient temperature. The observable change in solution's appearance, coupled with emergence of pale white precipitate, indicated the formation of ZnO precursor species. The precipitated nanoparticles were centrifuged at 6000 rpm for 10 minutes and washed three times with distilled water to remove residual ions and phytochemical impurities. The purified precipitate was subsequently dried in a hot air oven at 80 °C for 8 hours to obtain stable ZnO nanoparticles. All synthesis procedures were performed under identical conditions to ensure reproducibility of the nanoparticle formation (Khan *et al.* 2025b). The ZnO nanoparticles were later employed as catalysts for the conversion of *p*-nitrophenol to *p*-aminophenol and for degradation of several organic dyes.

2.4 Nitrophenol to Aminophenol

Biosynthesized ZnO nanoparticles (ZnO NPs) were utilized as catalyst for reduction of the PNP to PAP at inclusion of sodium borohydride. Initially, 1 mmol of PNP was dissolved in 1.85 mL of ultrapure water, by inclusion of 0.15 mL of 0.01 mmol $NaBH_4$ solution. The introduction of $NaBH_4$ caused reaction mixture to promptly turn vivid yellow, indicating the formation of *p*-nitrophenolate ion. Subsequently, 0.5 mg and 1 mg of ZnO catalyst were incorporated into the reaction mixture, and the reduction process was observed by UV spectroscopy at regular intervals. The progressive decline in the distinctive absorption peak of *p*-nitrophenolate (~400 nm) and concurrent emergence of peak associated with *p*-aminophenol (~300 nm) validated the successful catalytic reduction.

2.5 Catalytic Degradation of Organic Dyes

In catalytic reduction experiments, 9.75 mL of a 50 ppm aqueous MO solution was placed in a beaker. Then, 0.25 mL of 0.08 M $NaBH_4$ was added at ambient conditions. Subsequently, 1 mg of biosynthesized ZnO nanoparticles was introduced into the reaction mixture, and the solution was permitted to react at ambient temperature. At consistent time intervals, aliquots of reaction mixture were extracted and examined by UV spectrophotometer. The progressive decline of absorption peak strength of MO, along with a noticeable colour change of the solution, validated the catalytic reduction process. Identical experimental approach was utilized for degradation of additional organic dyes, MB and CR (Sanjeev *et al.* 2024). All catalytic degradation experiments were conducted in triplicate to ensure the reproducibility and reliability of the obtained results. The reported degradation efficiencies represent the average values obtained from three independent experiments, and

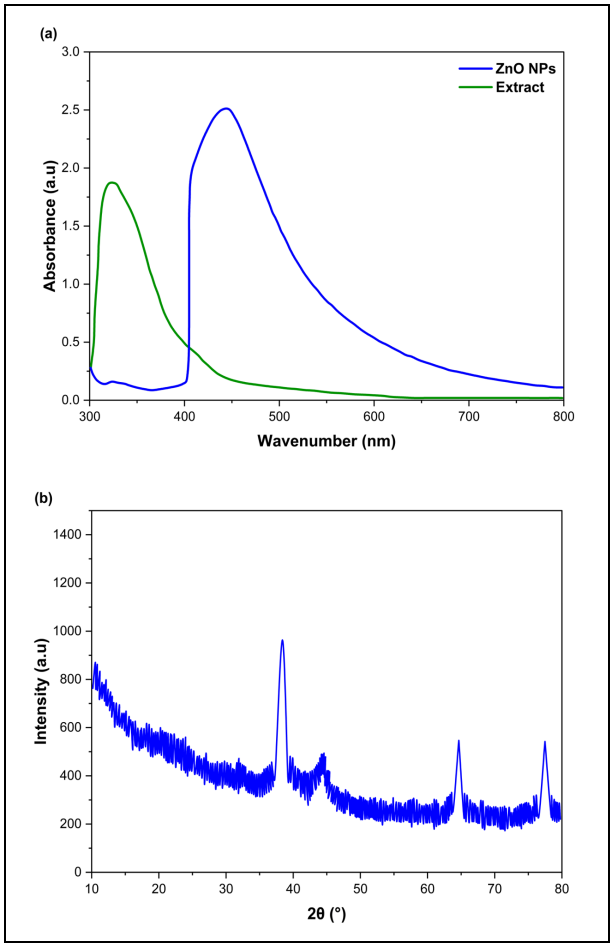
the variation among the repeated measurements was found to be minimal (±2%).

2.6 Characterization of ZnO Nanoparticles

The structural and optical properties of the synthesized ZnO nanoparticles were analyzed using several characterization techniques. UV–Visible absorption spectra were recorded in the wavelength range 200–800 nm using a UV–Vis spectrophotometer. X-ray diffraction (XRD) analysis was performed using Cu Kα radiation (λ = 1.5406 Å) operating at 40 kV and 30 mA with a scanning range of 20°–80°. Fourier transform infrared (FTIR) spectra were collected in the range 400–4000 cm^{-1} to identify functional groups associated with phytochemical capping agents. Morphological analysis was carried out using scanning electron microscopy (SEM), and elemental composition was confirmed using energy dispersive X-ray spectroscopy (EDX). Dynamic light scattering (DLS) measurements were conducted to determine the hydrodynamic particle size distribution and polydispersity index of the synthesized nanoparticles.

3. RESULTS AND DISCUSSION

3.1 Characterization of ZnO NPs



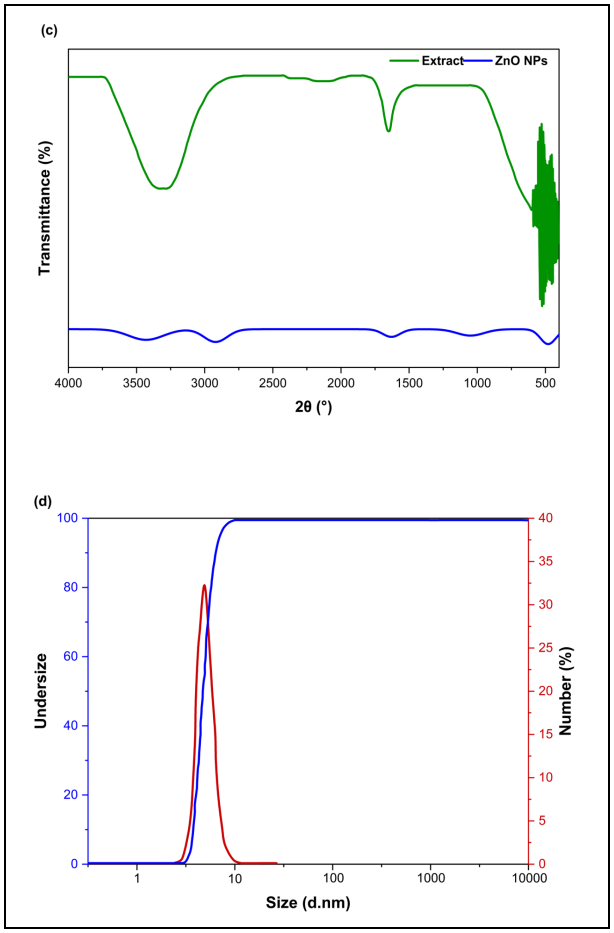


Fig. 2: (a) UV–Vis absorption spectrum confirming the formation of ZnO nanoparticles with a characteristic absorption peak around 432 nm; (b) XRD pattern showing the crystalline ZnO structure; (c) FTIR spectrum indicating the phytochemical functional groups involved in nanoparticle stabilization; and (d) DLS analysis showing the average nanoparticle size distribution

The UV spectrum exhibited a band at 432 nm, showing formation of ZnO using *Azadirachta indica* leaf extract. The band due to the leaf extract content was detected at 443 nm. The FT-IR spectra (Figure 2c) exhibit peak at 3315.08 cm^{-1}, showing the inclusion of -OH functionality, while the peak at 1647.19 cm^{-1} signifies the formation of a carbonyl group. The XRD examination reveals the structural characteristics and crystalline material phase. The ZnO nanoparticles exhibited Miller indices of (111), (200), (220), and (311), signifying an FCC structure with corresponding angles at 38.45°, 44.51°, 64.69°, and 77.58°. The observed peaks corresponded precisely with the documented data, and the extract facilitated the reduction of Zn to ZnO while stabilizing the synthesized zinc nanoparticles. Dynamic light scattering is a rapid and non-destructive method used to determine the dispersion of particles in suspensions and liquids. Fig. 2d illustrates that mean

diameter of hydrodynamic size of biosynthesized ZnO nanoparticles generated from *Azadirachta indica* leaf was 10 nm at a Zn concentration of 30 mM. The PDI score of 0.12 indicates that particles generated were singular and scattered.

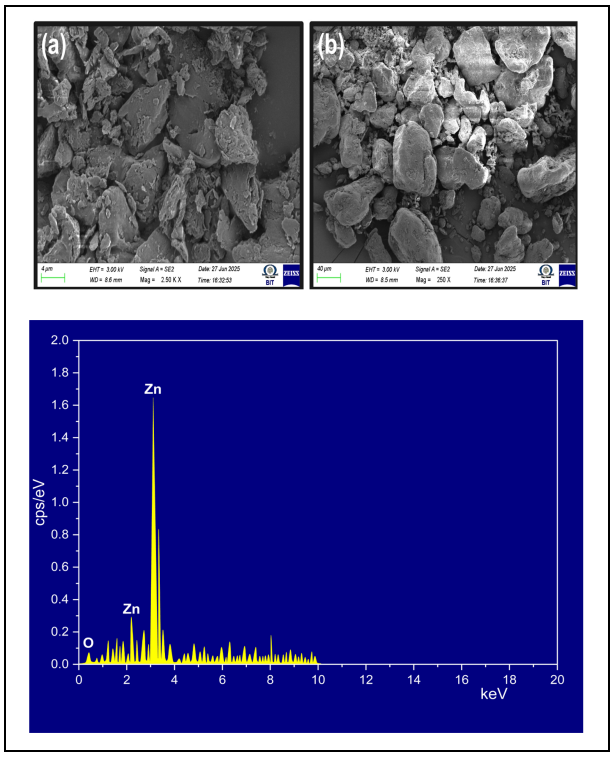


Fig. 3: (a,b) SEM images showing predominantly spherical ZnO nanoparticles with slight agglomeration; and (c) EDX spectrum confirming the elemental presence of zinc and oxygen in the synthesized nanoparticles

The morphology of the synthesized ZnO nanoparticles using *Azadirachta indica* leaf extract was examined by SEM analysis, revealing that the green-synthesized ZnO nanoparticles were homogeneous and spherical, with an average diameter of 50–100 nm. Elemental analysis was conducted using EDX, as illustrated in Fig. 3c. The EDX spectrum exhibits prominent and identifiable peaks associated with zinc, notably at 3 keV, indicative of zinc Lα emission line. This verifies effective synthesis and existence of elemental zinc in the nanoparticles. In prior investigations that the silver nanoparticles synthesized by *Azadirachta indica* leaf extract were confirmed by SEM images showed predominantly with slight agglomeration and uniform nanoscale distribution. The morphology confirms effective phytochemical-mediated stabilization and successful green synthesis (Shobana *et al.* 2025).

3.2 Catalytic Dye Reduction

Sulfated dyes such as MO and CR constitute hazardous waste generated in dye industry. Conversely, MB is a textile industry effluent difficult to eliminate due to its polar groups and aromatic rings, which hinder degradation. Consequently, the degradation were concentrated utilizing reducing agents like sodium borohydride. Reducing chemicals alone are incapable of reducing or degrading the dyes; they necessitate metal catalysts. Consequently, the environmentally friendly chemical production of ZnO NPs were employed for reduction of CR, MB and MO (Sharma *et al.* 2022). The diazo and azo groups at CR and MO were most direct approaches for degrading chromatic contaminants.

3.3 Catalytic Reduction of MO

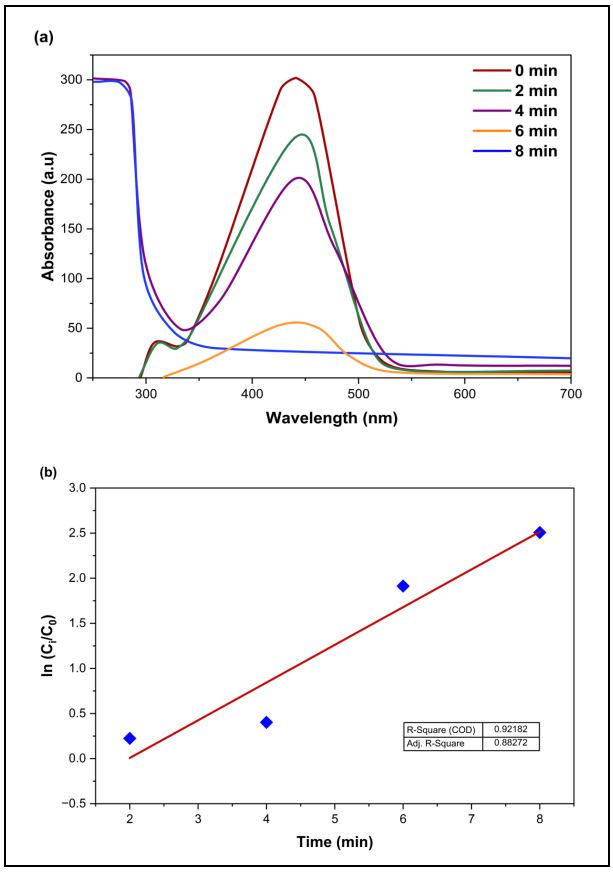


Fig. 4: (a) UV–Vis spectral changes during the catalytic reduction of methyl orange, showing a progressive decrease in the absorption peak at 442 nm; (b) pseudo-first-order kinetic plot confirming the linear relationship between ln(C_0/Ct) and reaction time

Initially, $NaBH_4$ acted as a catalyst for the degradation of methyl orange dye; however, its inability to alter the solution's color indicates that $NaBH_4$ alone cannot degrade the azo bond in methyl orange. Subsequently, 1 mg of ZnO nanoparticles was added to the solution. The intensity of the absorption peak at 442 nm progressively decreased, resulting in the orange solution becoming colorless. This signifies that the ZnO nanoparticles successfully reduced the azo bond in

methyl orange, achieving a degradation efficiency of 92%. Fig. 4b illustrates the linear correlation between ln(C_0/Ct) and reaction time, which was used to monitor the progression of the reduction reaction. The linear relationship indicates pseudo-first-order kinetics at ambient temperature, with a rate constant of 0.9218. The crystalline ZnO showed promising optical properties and potential for degradation of methyl orange (Suresh *et al.* 2022).

3.4 Catalytic Reduction of Congo Red Dye

The catalytic reduction mechanism involves the transfer of electrons from the reducing agent sodium borohydride ($NaBH_4$) to the dye molecules through the surface of ZnO nanoparticles. In the absence of a catalyst, direct electron transfer between $NaBH_4$ and the dye molecules is kinetically unfavorable. ZnO nanoparticles act as an electron relay system, facilitating the transfer of electrons from BH_4^- ions to the chromophoric groups of dye molecules. The high surface area of ZnO nanoparticles allows adsorption of both dye molecules and BH_4^- ions on the catalyst surface, enabling efficient electron transfer and rapid reduction of azo bonds in dyes. This process ultimately leads to the breakdown of the dye structure and discoloration of the solution.

The ZnO nanoparticles were employed to investigate the catalytic degradation of Congo red dye in the presence of $NaBH_4$, as illustrated in Fig. 5a. An absorption peak at 475 nm was observed during the reduction of Congo red, as indicated by the UV–visible spectra. The dye diminishes over time, signifying its slow breakdown. In previous studies, unmodified *Azadirachta indica* leaf powder characterized by SEM and FTIR was applied for Congo red adsorption. The process followed pseudo-first-order kinetics and Freundlich isotherm behavior, confirming efficient dye removal (Javed *et al.* 2024). The decrease in absorbance intensity indicates that the ZnO nanoparticles efficiently facilitate electron transport from NaBH4 to dye molecule. Reaction approaches completion in 16 minutes, attaining roughly 96% degradation. Reaction time was calculated by ln (Ci/C0), demonstrating pseudo-first-order by correlation coefficient 0.8735, validating model's applicability. The rate constant (k) for reduction process was 0.8735 min^{-1}, signifying catalytic reaction enabled elevated surface reactivity of ZnO nanoparticles.

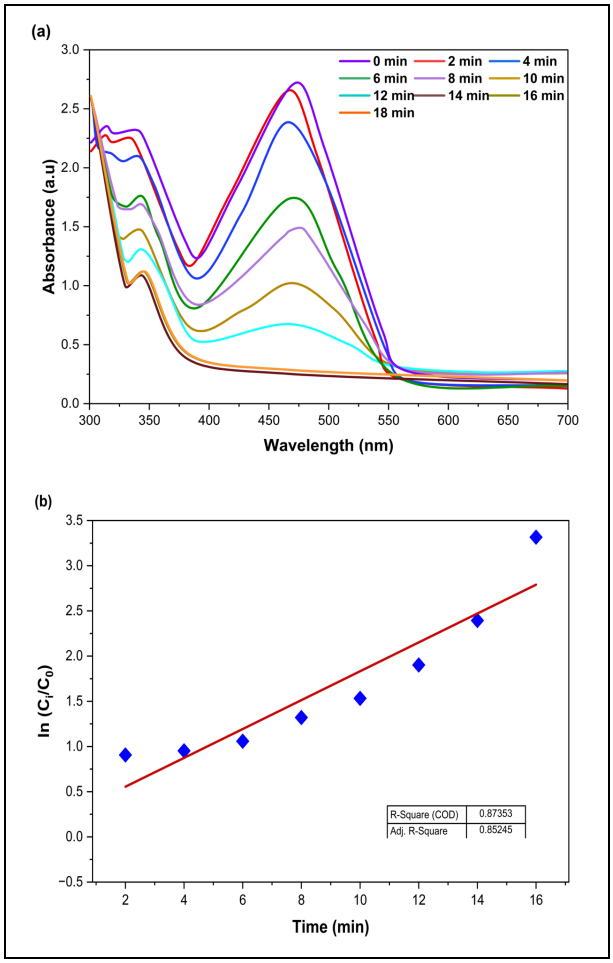


Fig. 5: (a) UV–Vis spectral changes indicating the catalytic degradation of Congo red with decreasing absorbance at 475 nm; and (b) pseudo-first-order kinetic plot demonstrating the reaction rate behavior

3.5 Catalytic Reduction of Methyl Blue

The ZnO NPs were used as a catalyst in the degradation of MB dye in presence of sodium borohydride. The ZnO nanoparticles efficiently degraded methylene blue dye by 95% within 10 minutes, following pseudo-first-order kinetics with a rate constant of 0.8676. As reported in previous studies, green synthesis of ZnO/MgO nanocomposites using *Azadirachta indica* leaf extract was confirmed through SEM, EDX, XRD, and UV-Vis. The nanocomposites showed enhanced photocatalytic degradation of MB and potential for CR and methyl orange remediation (Poonam *et al.* 2023).

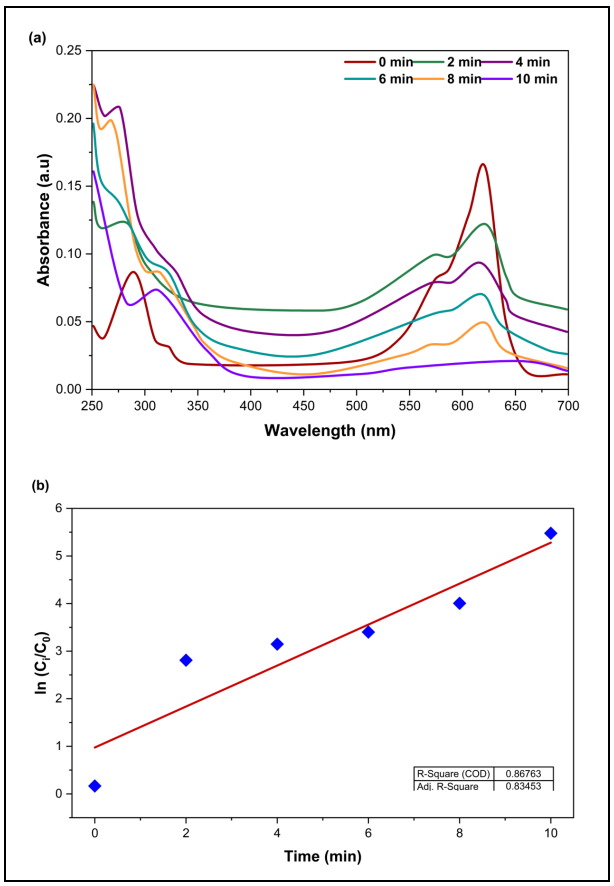


Fig. 6: (a) UV–Vis spectral evolution showing the gradual reduction of methylene blue dye; and (b) pseudo-first-order kinetic plot indicating efficient catalytic degradation

Figure 7 illustrates the degradation percentages of MB (97.82%), CR (98.29%) and MO (95.35%). The high volume-to-surface ratio of ZnO nanoparticles offers increased catalytic sites and reduced activation energy. Thus, the surface interaction between the reactant and ZnO nanoparticles may be responsible for catalytic degradation of organic dyes.

Several studies have reported degradation efficiencies of 80–95% for dyes such as methylene blue and Congo red within reaction times ranging from 30 to 180 minutes (Medina-Acosta *et al.* 2024; Subramani *et al.* 2025). In contrast, the ZnO nanoparticles synthesized using *Azadirachta indica* leaf extract in the present study achieved degradation efficiencies of 97.82% for methylene blue, 98.29% for Congo red, and 95.35% for methyl orange within 8–16 minutes, indicating significantly faster catalytic activity. This improved performance can be attributed to the small particle size, high surface area, and phytochemical-mediated surface functionalization of the ZnO nanoparticles, which enhance catalytic active sites and electron transfer efficiency.

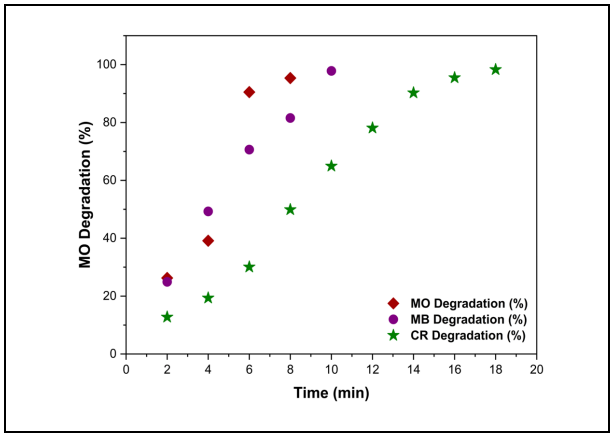


Fig. 7: Time-dependent catalytic degradation efficiencies of MO, MB, and CR using biosynthesized ZnO nanoparticles, demonstrating rapid dye removal within short reaction times

Table 1. Pseudo-first-order kinetic parameters for catalytic dye degradation

Dye	Rate Constant k (min^{-1})	Correlation Coefficient (R^2)	Reaction Time (min)	Degradation Efficiency (%)
Methyl orange	0.9218	0.92	8	95.35
Congo red	0.8735	0.87	16	98.29
Methylene blue	0.8676	0.91	10	97.82

Table 1 summarizes the catalytic degradation efficiencies of MO, MB and CR using neem-mediated ZnO nanoparticles. The ZnO nanoparticles were found to possess significant stability and catalytic efficacy, rendering them highly promising as catalysts for cleaning of wastewater and industrial effluents tainted by organic dyes.

3.6 Conversion of Nitrophenol to Aminophenol

To evaluate the catalytic activity ZnO nanoparticles, PNP was catalytically reduced to PAP using $NaBH_4$. Reaction was executed by combining 0.15 mL of $NaBH_4$, 0.5 mg of ZnO nanoparticles and 1.85 mL of PNP, in a UV cuvette, with the reaction progress monitored at specified time intervals. *p*-Nitrophenol shows absorption at 306 nm. The deprotonation of the OH of PNP, which results in the formation of the *p*-nitrophenolate, causes absorption peak shift from 306 to 400 nm, as a result of the introduction of $NaBH_4$. The light-yellow coloration of PNP transitioned to a yellow color. During the reaction, the peak intensity of the nitrophenolate ion at 400 nm progressively diminished, while a new peak appeared at 306 nm, signifying the formation of PAP. Moreover, the isosbestic points at 250 and 350 nm confirmed the formation of PAP without

byproducts, and the yellow solution eventually became colorless. Figure 8b presents a kinetic analysis by displaying ln (Ct/C0) with time, with Ct and C0 representing the absorbance levels at 400 nm at time zero, respectively.

The catalytic degradation kinetics were evaluated using a pseudo-first-order kinetic model, which is commonly applied for catalytic dye reduction reactions. The relationship between dye concentration and reaction time was expressed using the equation $\ln(C_0/Ct) = kt$, where C_0 represents the initial dye concentration, Ct represents the concentration at time t, and k is the apparent rate constant. The linear relationship observed in the $\ln(C_0/Ct)$ *versus* time plots confirms that the catalytic degradation follows pseudo-first-order kinetics, indicating efficient catalytic activity of the ZnO nanoparticles.

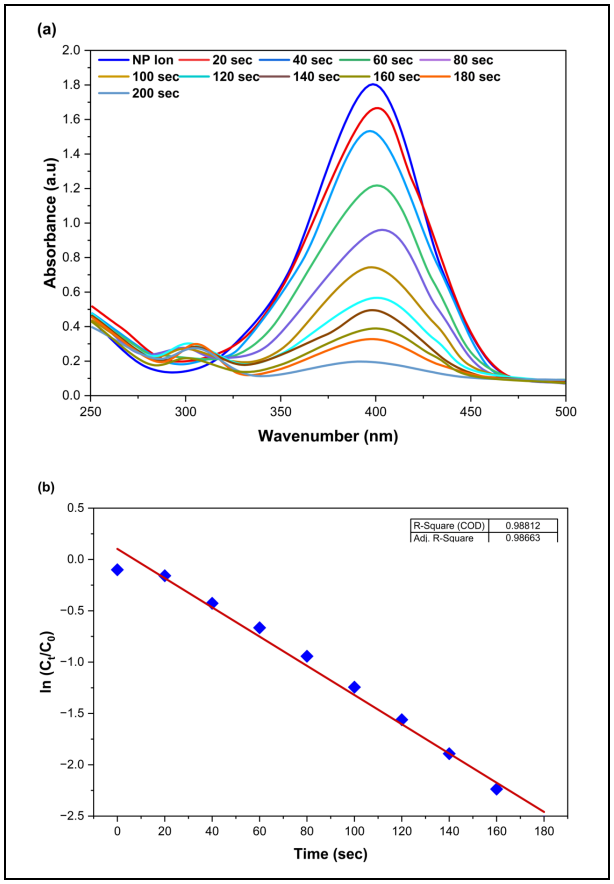


Fig. 8: (a) Ultraviolet–vis spectrum of 4-NP (0.5mg) reduction and (b) Kinetic analysis of ZnO-catalyzed 4-NP reduction

A comparable trend was observed in Fig. 9 for the reaction conducted using 1 mg of ZnO nanoparticles. Figure 9a demonstrates a much quicker spectral evolution, with the complete elimination of the 400 nm peak occurring within 120 seconds. The kinetics of the reduction process were analyzed by spectrophotometry, which revealed increased catalytic activity at higher concentrations. The kinetic plot in Fig. 9b exhibits a linear relationship with a high R^2 value of 0.9919, confirming pseudo-first-order kinetics. The elevated rate constant with increased ZnO nanoparticle dosage underscores the direct correlation between catalyst concentration and catalytic efficiency.

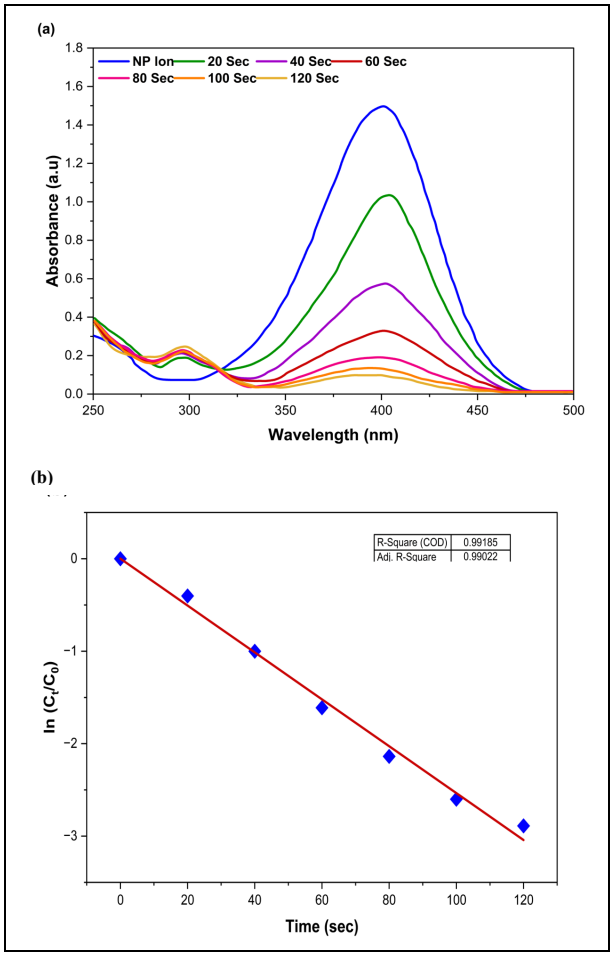


Fig. 9: (a) Ultraviolet–vis spectrum of 4-NP (1mg) reduction and (b) Kinetic analysis of ZnO-catalyzed 4-NP reduction

The notable rise in reaction rate at higher catalyst loading is due to expanded surface area for electron transfer activities. The absence of side-product peaks and the presence of distinct isosbestic points in the spectra validate the selective transformation of PNP to PAP, establishing the system as an effective and environmentally friendly method for nitroaromatic reduction.

4. CONCLUSIONS

Azadirachta indica -mediated green synthesis of ZnO nanoparticles using *Azadirachta indica* leaf extract provides a simple, economical, and environmentally sustainable route for synthesizing effective catalytic

nanomaterials. Structural and morphological analyses using XRD, UV–Vis, FTIR, DLS, SEM, and EDX confirmed the successful formation of predominantly spherical ZnO nanoparticles with particle sizes below 100 nm. The synthesized nanoparticles exhibited excellent catalytic performance toward the reduction of organic pollutants. High degradation efficiencies of 95.35% for methyl orange, 97.82% for methylene blue, and 98.29% for Congo red were achieved within short reaction times, while *p*-nitrophenol was rapidly converted to *p*-aminophenol within approximately 2–4 minutes in the presence of $NaBH_4$. The enhanced catalytic performance is attributed to the high surface area and active catalytic sites of the biosynthesized ZnO nanoparticles, which facilitate efficient electron transfer during the reduction process. Future research may focus on evaluating the reusability and long-term stability of the ZnO catalyst, as well as investigating its performance in real industrial wastewater systems containing mixed pollutants. Such studies would further validate the practical applicability of neem-mediated ZnO nanoparticles for large-scale environmental remediation and wastewater treatment.

FUNDING

This research received no specific grant from any funding agency in the public, commercial, or not-for-profit sectors.

CONFLICTS OF INTEREST

The authors declare that there is no conflict of interest.

COPYRIGHT

This article is an open-access article distributed under the terms and conditions of the Creative Commons Attribution (CC BY) license (http://creativecommons.org/licenses/by/4.0/).



REFERENCES

Ansari, A., Ali, A., Khan, N., Saad, U. M. and Owais, M., Synthesis of steroidal dihydropyrazole derivatives using green ZnO NPs and evaluation of their anticancer and antioxidant activity, *Steroids*, 188 109113(2022). https://doi.org/10.1016/j.steroids.2022.109113

Arayesh, M. A., Kianfar, A. H. and Mohammadnezhad, G., Synthesis of $Fe_3O_4/ZrO_2/ZnO$ nanoparticle for enhancing visible light photocatalytic and antibacterial activity, *J. Taiwan Inst. Chem. Eng.*, 153, 105213(2023). https://doi.org/10.1016/j.jtice.2023.105213

Barrios-Navarro, F. A., Vilchis-Néstor, A. R. V. and Morales, P. A. L., Photocatalytic degradation of organic dyes in water using semiconductor ZnO nanoparticles synthesized using Crataegus mexicana extract, *Mater. Chem. Phy.*, 318, 129302(2024). https://doi.org/10.1016/j.matchemphys.2024.129302

Behera, M., Othman, A. F., Chakrabortty, S., Nayak, J., Banerjee, S., Kumar, R., Jeon, B. -H. and Tripathy, S. K., $CuO/TiO_2/ZnO$ NPs Anchored Hydrogen Exfoliated Graphene: To Comprehend the Role of Graphene in Catalytic Reduction of p-Nitrophenol, *ACS Omega*, 8(45), 42164–42176 (2023). https://doi.org/10.1021/acsomega.3c03859

Doan, L., Tran, K., Huynh, K. G., Nguyen, T. T. T., Nguyen, T. D. M., Tang, L. V. H., Truong, M. L. T., Le, Q. N. and Huynh, A. H., Surface modifications of graphitic carbon nitride with metal particles and polymer blend as antibacterial and dye removal agents, *Sci. Rep.*, 15(1), 38087(2025). https://doi.org/10.1038/s41598-025-21829-2

Fuentes, J. A. V, Martinez, D. K. M., Ortiz, L. M. O., Vilchis-Néstor, A. R. V. and Morales, P. A. L., Sustainable synthesis of ZnO nanoparticles from Brickellia cavanillesii extract with enhanced photocatalytic and antimicrobial properties, *Res. Chem. Intermedi.*, 51(10), 5425–5449 (2025). https://doi.org/10.1007/s11164-025-05720-3

Furhan and Ramesan, M. T., Development of conductive poly (para-aminophenol)/zinc oxide nanocomposites for optoelectronic devices, *Polym. Bulletin*, 80(6), 6405–6432 (2023). https://doi.org/10.1007/s00289-022-04373-1

Furhan and Ramesan, M. T., Zinc oxide reinforced poly(para-aminophenol) nanocomposites: Structural, thermal stability, conductivity and ammonia gas sensing applications, *J. Macromol. Sci., Part A: Pure Appl. Chem.*, 59(10), 675–688 (2022). https://doi.org/10.1080/10601325.2022.2111262

Javed, T., Thumma, A., Uddin, A. N., Akhter, R., Taj, M. B., Zafar, S., Baig, M. M., Shah, S. S. A., Wasim, M., Abid, M. A., Masood, T., Jilani, M. I. and Batool, M., Batch adsorption study of Congo Red dye using unmodified *Azadirachta indica* leaves: isotherms and kinetics, *Water Practice Technol.*, 19(2), 546–566 (2024). https://doi.org/10.2166/wpt.2024.020

Khan, A., Ahmad, S. J. N., Jafir, M., Ahmad, A., Irfan, M., Qasim, M., Ahmad, J. N., Sabir, M. A., Maqsood, M. F., Rehman, A., Alsakkaf, W. A. A. and Ali, H. M., Green Synthesis, Characterization, and Effect of Zinc Oxide Nanoparticles on Wheat (Triticum Aestivum L.) Under Cadmium Stress, *J. Soil Sci. Plant Nutri.*, 25(4), 8995–9010 (2025a). https://doi.org/10.1007/s42729-025-02708-1

Khan, S. B., Ismail, M., Bakhsh, E. M. and Asiri, A. M., Design of simple and efficient metal nanoparticles templated on ZnO-chitosan coated textile cotton towards the catalytic reduction of organic pollutants, *J. Indus. Tex.*, 51(1), 1703–1728 (2022). https://doi.org/10.1177/1528083720931481

Khan, S., Ullah, A., Ahmad, I., Sher, A., Rehman, G., Hayat, K., Ahmad, M., Shah, S. K. and Gunnella, R., Therapeutic potential of green-synthesized ZnO from *Azadirachta indica*: a study on anti-diabetic, anti-inflammatory, and anti-bacterial activities, *J. Sol-Gel Sci. Technol.*, 116(2), 1581–1596 (2025b). https://doi.org/10.1007/s10971-025-06938-8

Krishnaiah, C. V. and Kumar, B. D., Green synthesis of ZnO-NiO nanocomposite via neem leaf extract for electrochemical sensing and photocatalytic applications, *Ionics*, 31(11), 12227–12243 (2025). https://doi.org/10.1007/s11581-025-06647-w

Kumar, P. and Thakur, N., Examination of seed germination process and assess phytotoxicity in Vigna radiata (Mung bean) and Allium cepa (Onion) using triple-doped green hematite nanoparticles and their photocatalytic potential, *Environ. Sci. Pollut. Res.,* (2025). https://doi.org/10.1007/s11356-025-36735-3

Kumar, P., Kumar, S., Tapwal, A., Nimesh, S. and Thakur, N., Water purification and biological efficacy of green synthesized Co/Zn-Doped α-Fe_2O_3 nanoparticles, *Sustain. Chem. Environ.*, 8, 100160(2024). https://doi.org/10.1016/j.scenv.2024.100160

Kumar, P., Thakur, N., Tapwal, A. and Kumar, S., Enhancing the adsorption capacity of green/chemical synthesized hematite nanoparticles by copper doping: removal of toxic Congo red dye and antioxidant activity, *Appl. Nanosci.,* 13(9), 6591–6604 (2023). https://doi.org/10.1007/s13204-023-02943-x

Lal, R., Sharma, A., Gour, T., Agarwal, L. K., Sharma, Y. K., Chetri, S. P. K., Kumar, R., Kumar, P., Sharma, A. K. and Sharma, K., Biogenic production of eco-friendly Arjuna-ZnO NPs for sunlight-activated efficient degradation of organic dyes of high commercial usage, *J. Saudi Chem. Soc.*, 28(3), 101851(2024). https://doi.org/10.1016/j.jscs.2024.101851

Magaña-Chavez, C. A., Villegas-Fuentes, J. A., Nava, O. J., Vilchis-Néstor, A. R. V. and Morales, P. A. L., Green synthesis of semiconductor nanoparticles (ZnO, CuO, and SnO_2) using Physalis philadelphica peel extract: characterization and photocatalytic studies on five organic dyes, *J. Mater. Sci. Mater. Electron.*, 36(26), 1728(2025). https://doi.org/10.1007/s10854-025-15811-x

Manzoor, A., Elboughdiri, N., Zafar, S., Khan, M. I., Manzoor, S., Suleman, J., Zafar, A. M., Aslam, S., Rajput, R., Shanableh, A., Shuja, R., Ahmad, F. Shahida, S., Preparation of composite of bentonite clay and *Azadirachta indica* (neem) leaves powder for the removal of Congo red from an aqueous solution, *Desalin. Water Treat.*, 314, 241–250 (2023). https://doi.org/10.5004/dwt.2023.30094

Medina-Acosta, M., Chinchillas-Chinchillas, M. J., Garrafa-Gálvez, H. E., García-Maro, C. A., Rosas-Casarez, C. A., Lugo-Medina, E., Morales, P. A. L., and Soto-Robles, C. A., Photocatalytic Degradation of Four Organic Dyes Present in Water Using ZnO Nanoparticles Synthesized with Green Synthesis Using Ambrosia ambrosioides Leaf and Root Extract, *Proce.*, 12(11), 2456(2024). https://doi.org/10.3390/pr12112456

Nandana, E., Dwivedi, A. H. and Nidheesh, P. V., Role of biochar in superoxide-dominated dye degradation in catalyst-activated peroxymonosulphate process, *Chemosphere*, 356, 141945(2024). https://doi.org/10.1016/j.chemosphere.2024.141945

Ounis, D. Y., Peppel, T., Sebek, M., Strunk, J. and Houas, A., Green Synthesis of Photocatalytically Active ZnO Nanoparticles Using Chia Seed Extract and Mechanistic Elucidation of the Photodegradation of Diclofenac and p-Nitrophenol, *Catal.*, 15(1), 4(2025). https://doi.org/10.3390/catal15010004

Poonam, D., Honey, S. and Indu, J., Green and Facile Approach for the Synthesis of ZnO/MgO Nanocomposite using *Azadirachta indica* Leaf Extract: Characterization and Photocatalytic Activity, *Res. J. Chem. Environ.*, 27(6), 51–57 (2023). https://doi.org/10.25303/2706rjce051057

Quevedo-Robles, R. V., Santana-Camacho, D., Vilchis-Néstor, A. R. V. and Morales, P. A. L., Role of natural extracts on the synthesis and properties of semiconductor nanoparticles of ZnO applied in water treatment by photocatalytic processes, *J. Mater. Sci. Mater. Electron.*, 35(11), 757(2024). https://doi.org/10.1007/s10854-024-12505-8

Rani, N., Rawat, K., Saini, M., Shrivastava, A., Kandasamy, G., Saini, K. and Maity, D., Rod-shaped ZnO nanoparticles: synthesis, comparison and in vitro evaluation of their apoptotic activity in lung cancer cells, *Chem. Pap.*, 76(2), 1225–1238 (2022). https://doi.org/10.1007/s11696-021-01942-y

Raza, A., Ashraf, A., Ali, S., Bashir, F., Farrukh, M. A., Naseem, F. and Shahwar, D. E., Assessing the Impact of NaOH on Green Synthesis of Zinc-Based Nanoparticles Using Onion Extract and Exploring Their Photocatalytic, Antibacterial, and Antioxidant Potentials, *Chem. Select*, 10(23), e00253(2025). https://doi.org/10.1002/slct.202500253

Sanjeev, N. O., Manjunath, M. S. and Valsan, A. E., *Azadirachta indica* leaf extract based green-synthesized ZnO nanoparticles coated on spent tea waste activated carbon for pharmaceuticals and personal care products removal, *Environ. Res.*, 252, 119047(2024). https://doi.org/10.1016/j.envres.2024.119047

Sharma, B. K., Mehta, B. R., Shah, E. V, Chaudhari, V. P., Roy, D. R. and Roy, S., Green Synthesis of Triangular ZnO Nanoparticles Using *Azadirachta indica* Leaf Extract and Its Shape Dependency for Significant Antimicrobial Activity: Joint Experimental and Theoretical Investigation, *J. Cluster Sci.*, 33(6), 2517–2530 (2022). https://doi.org/10.1007/s10876-021-02145-x

Shobana, N., Prakash, P., Samrot, A. V, Saigeetha, S., Dhiva, S., Thirumurugan, A., Rajalakshmi, D., Emilin, R. R. E. and Abirami, S., Natural biopolymer mediated green synthesis of silver nanoparticles and its applications in environmental remediation, *Biomass Convers. Biorefine.*, 15(1), 531–544 (2025). https://doi.org/10.1007/s13399-024-05282-1

Slathia, S., Gupta, T. and Chauhan, R. P., Green synthesis of Ag–ZnO nanocomposite using *Azadirachta indica* leaf extract exhibiting excellent optical and electrical properties, *Physica B: Condens. Matter.*, 621, 413287(2021). https://doi.org/10.1016/j.physb.2021.413287

Subramani, K., Ganeshan, J. K. S., Srinivasan, S., Mohanasundaram, N. V. T. and Incharoensakdi, A., Hydrothermally and green synthesized TiO_2 nanoparticles with high photocatalytic textile industry dye degradation, antibacterial and antioxidant activities, *J. Alloys Compds*, 1017, 179068(2025). https://doi.org/10.1016/j.jallcom.2025.179068

Suresh, M., Vennila, J. and Ramanathan, P., Plant-Based Zno Nanomaterials and their Optical Properties, *Rasayan J. Chem.*, 300–306 (2022). https://doi.org/10.31788/RJC.2022.1558048

Venkata, K. C. and Behara, D. K., Photocatalytic and electrochemical sensor studies of CuO-ZnO nanocomposite synthesized via green combustion using neem leaf extract, *Mater. Sci. Technol.,* 67107(2025). https://doi.org/10.1177/02670836251367107